J. Fluid Mech. (1971), *vol.* 49, *part* 2, *pp.* 209–222
Printed in Great Britain

Infinite models for ciliary propulsion

By J. R. BLAKE

Department of Applied Mathematics and Theoretical Physics,
University of Cambridge

(Received 11 December 1970)

This paper discusses two infinite length models (planar and cylindrical) for ciliary propulsion of microscopic organisms. Through the concept of an extensible envelope (instantaneous surface covering the numerous cilia) over the organism, we consider a small amplitude analysis for the velocity of propulsion. A comparison of the velocities of propulsion for the infinite models reveals that they are just over twice that obtained for the finite spherical model (Blake 1971). This indicates that planeness is more important than finiteness, as the solution for typical micro-organisms (e.g. disk-shaped) should occur somewhere between these two models. The maximum velocity of propulsion obtained is one quarter of the wave velocity; that inferred for *Opalina*, the organism modelled, is nearly one fifth of the wave velocity. Associated shapes of the surface and paths of movement of the tips of the cilia are illustrated.

1. Introduction

Few studies from the hydrodynamical point of view have been made on ciliary motion. In this paper, we consider two infinite length models for ciliary propulsion and compare them with the finite length model given in a previous paper (Blake 1971). Comparisons are also made with the actual velocities of the ciliated organisms.

Many small microscopic organisms are propelled by high concentrations of cilia on the surface of the organism. The cilia are located in rows along and across the organism, while the organism is propelled in the opposite direction to that of the effective beat of the cilia. The movements of adjacent cilia are slightly out of phase (metachronism), and the direction in which they are out of phase determines the name of the type of metachronism exhibited by the organism. This metachronism viewed from above (or side on), appears as a wave passing over the organism. For these models we take an extensible 'envelope' over the tips of the numerous undulating cilia, thus replacing the individuality of the cilia by a progressive waving envelope. This approximation is perhaps only valid in one type of metachronism, that of the symplectic type, which occurs when the cilia beat in the same direction as that of the wave. We would expect, and in fact find, the cilia to be bunched close together in this type of metachronism throughout the complete cycle of the beat. The no-slip condition is imposed on the extensible envelope, with no allowance being made for blowing or sucking, which may occur in some organisms.

As the organisms are very small, and velocities (both wave and propulsive) small also, the Reynolds numbers are extremely low, thus enabling us to use the creeping flow equations of motion. Taylor (1951) was the first to show that propulsion of a microscopic organism can occur when the viscous stresses are dominant.

Through the use of axisymmetric potential theory (Weinstein 1953) we formulate two problems together, (i) the two-dimensional waving sheet, and (ii) axisymmetric waving cylinder, with the waving bodies propelling themselves through the infinite liquid domain (see figure 1). Burns & Parkes (1967) considered the flow in the interior of the 'tubes' (i.e. general term used for both (i) and (ii)), whereas in this problem the flow field outside the 'tubes' is of interest. However, in this paper we will also consider longitudinal movements as well as the transverse oscillations considered by Burns & Parkes. Otherwise, the actual mathematics is obtained by simply replacing the modified Bessel functions of the first kind $I_n(z)$, by those of the third kind $K_n(z)$ (Watson 1966). Taylor (1952) considered an infinite waving cylinder as a model for a flagellum, but the flow field in his model is not axisymmetric. The first model has previously been discussed by Taylor (1951), Reynolds (1965) and Tuck (1968). Taylor's model was an inextensible model of a transverse wave at zero Reynolds number. His inextensibility condition allows longitudinal movements to the second order; in fact a fixed point on the sheet moves through a figure-of-eight path in each period of oscillation. Reynolds introduces first-order movements in the longitudinal direction as well as the transverse by allowing the sinusoidal surface to strain. Tuck modified and simplified some of the earlier results, and considered both longitudinal and transverse oscillations separately. However, in the present paper, longitudinal and transverse oscillations acting together are assumed in the analysis throughout, and hence the envelope surface will be quite different from the sinusoidal shape employed in previous papers. The expressions for the velocity of propulsion and rate of working are obtained in more generality than previous approaches.

The strict validity of these models for ciliary propulsion at first sight is somewhat doubtful, for we are trying to model finite (small) length organisms by infinite models. The use of (i) and (ii) as models is justified because ciliated organisms tend to be elongated or flat, e.g. *Paramecium* or *Opalina* (so that a high ratio of surface area to volume can occur and hence a large number of cilia to propel the organism). Sheets of ciliated surface that are effectively infinite also occur on the ciliated epithelia of multi-cellular animals. These models may then be an appropriate approximation if we suppose that end effects of the organism are negligible, and that in the middle of the organism the waves passing over it are similar to those over an infinite sheet. In any case we may hope to learn something of the influence of finite size by comparing the present infinite models with the finite spherical model (Blake 1971).

In this type of problem it is important for us to define the frame of reference in which the calculations will be carried out. We choose the reference frame to be one where the waves are stationary, which in our notation will be represented by the z co-ordinate. This co-ordinate is defined by $z = kx + \sigma t$, which in the

x co-ordinate system (fixed in the moving organism) gives for wave-like functions a velocity of wave propagation in the negative x direction of magnitude $c = \sigma/k$. In the z co-ordinate system the velocity of the fluid at infinity will be $c - U$, where U is the velocity of propulsion of the sheet.

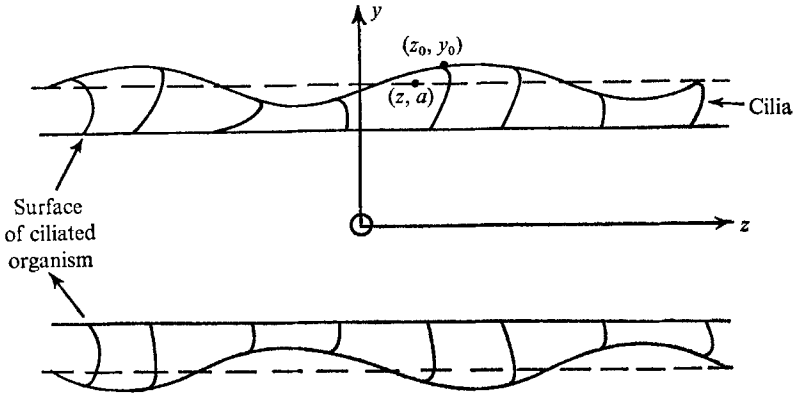

FIGURE 1. Diagram illustrates envelope over cilia. Co-ordinates (z_0, y_0) represent envelope, (z, a) mean position. Velocity at infinity, $u = c - U$.

2. Equations of motion

The equations of motion for this problem are those for creeping flow,

$$\nabla p = \mu \nabla^2 \mathbf{q}, \quad \nabla . \mathbf{q} = 0, \tag{1}$$

where p is the pressure, $\mathbf{q}$ the velocity vector, and μ the viscosity. We take small perturbations about a mean tube ($y = \pm a$) and then the problem may be reduced to solving the above equations, with the boundary conditions being velocities given on the mean tube (as distinct from the envelope). These velocities in terms of the perturbations are obtained later by a Taylor series expansion about the mean tube, as we know the velocities at the envelope surface due to the no-slip condition. This approach was used by Lighthill (1952) in his spherical model for propulsion at low Reynolds number. An alternative approach to satisfy the no-slip condition at the envelope surface is to expand the solution for the velocities in terms of the small perturbations and then equating this to the no-slip condition. From this we obtain an infinite set of linear equations which may be truncated to the required order of accuracy (see Burns & Parkes 1967). Both methods give the same solution, but the former approach appears to be easier for the order of magnitude to which we are working.

Using axisymmetric potential theory, the equation for the stream function ψ can be written in terms of

$$L_m = \frac{\partial^2}{\partial z^2} + \frac{\partial^2}{\partial y^2} - \frac{m}{y}\frac{\partial}{\partial y}, \tag{2}$$

as

$$L_m^2 \psi(z, y) = 0, \tag{3}$$

where $m = 0, 1$ depending on whether we are considering the two-dimensional tube or the axisymmetric cylinder, respectively.

In both cases a Fourier series expansion for $\psi(z, y)$ is taken, and for convenience a non-dimensional wave-number is used.

$$\psi(z, y) = \sum_{n=0}^{\infty} (f_n \cos nz + g_n \sin nz)\, \psi_n(y), \tag{4}$$

so that $\psi_n(y)$ satisfies the following ordinary differential equation:

$$D_{mn}^2 \psi_n = 0, \tag{5}$$

where
$$D_{mn} = \frac{d^2}{dy^2} - \frac{m}{y}\frac{d}{dy} - n^2 \quad (m = 0, 1;\ n = 1, 2, \ldots). \tag{6}$$

The boundary conditions for the z and y directional velocities on $y = a$ and in a frame of reference moving with the crests are

$$\left.\begin{aligned} u(z, a) &= A_0 + \sum_{n=1}^{\infty} (A_n \cos nz + B_n \sin nz), \\ v(z, a) &= \sum_{n=1}^{\infty} (C_n \cos nz + D_n \sin nz), \end{aligned}\right\} \tag{7}$$

which are the velocities at the mean radius of the tube. In the two-dimensional case the boundary conditions also need to be satisfied at $y = -a$. However, the upper ($y \geqslant a$) and the lower ($y \leqslant -a$) half planes reduce to the same problem, so we need only consider the upper half plane. We can also translate the tube wall, in the two-dimensional case, so that it coincides with the z axis thus making the analysis more compact.

The velocity components in terms of the stream function are

$$u = \frac{1}{y^m}\frac{\partial \psi}{\partial y}, \quad v = \frac{-1}{y^m}\frac{\partial \psi}{\partial z} \quad (m = 0, 1). \tag{8}$$

A representative solution for the two-dimensional waving plate at the translated origin is

$$\psi(z, y) = \beta_0 y + \sum_{n=1}^{\infty} [(\alpha_n + \beta_n y) \cos nz + (\gamma_n + \delta_n y) \sin nz]\, e^{-ny}, \tag{9}$$

whereas for the axisymmetric case

$$\begin{aligned} \psi(z, y) = \beta_0 y^2 + \sum_{n=1}^{\infty} [&(\alpha_n y K_1(ny) + \beta_n y^2 K_0(ny)) \cos nz \\ &+ (\gamma_n y K_1(ny) + \delta_n y^2 K_0(ny)) \sin nz]. \end{aligned} \tag{10}$$

From the above definitions of velocity in terms of the stream function, and the boundary conditions in terms of the surface coefficients on $y = a$, we then obtain for this co-ordinate system the following solutions for the z and y directional velocities. For (i), the velocities at (z, y) are,

$$u = c - U + \sum_{n=1}^{\infty} e^{-ny} [(A_n - n(A_n + D_n) y) \cos nz + (B_n - n(B_n - C_n) y) \sin nz], \tag{11}$$

$$v = \sum_{n=1}^{\infty} e^{-ny} [(D_n + n(A_n + D_n) y) \sin nz + (C_n - n(B_n - C_n) y) \cos nz], \tag{12}$$

and for (ii)

$$u = c - U + \sum_{n=1}^{\infty} \frac{1}{\phi(n)} [\cos nz \{K_0(ny)\,[2K_1A_n + na(K_1D_n + K_0A_n)]$$
$$- nyK_1(ny)\,[K_1A_n + K_0D_n]\} + \sin nz \{K_0(ny)\,[2K_1B_n + na(K_0B_n - K_1C_n)]$$
$$- nyK_1(ny)\,[K_1B_n - K_0C_n]\}], \tag{13}$$

and

$$v = \sum_{n=1}^{\infty} \frac{1}{\phi(n)} [\cos nz \{K_1(ny)\,[2K_0C_n + na(K_0B_n - K_1C_n)]$$
$$- nyK_0(ny)\,[K_1B_n - K_0C_n]\} + \sin nz \{K_1(ny)\,[2K_0D_n - na(K_1D_n + K_0A_n)]$$
$$+ nyK_0(ny)\,[K_1A_n + K_0D_n]\}], \tag{14}$$

where
$$\phi(n) = 2K_0(na)\,K_1(na) + na[K_0^2(na) - K_1^2(na)] \tag{15}$$

and K_0 and K_1 are Bessel functions of the third kind of zero and first order, of argument na, unless otherwise specified. The velocity of propulsion of the organism is ($c = \sigma$ for non-dimensional k),

$$U = c - A_0. \tag{16}$$

From the creeping flow equations we can calculate the pressure, and hence from this the surface stresses exerted by the organism on the fluid. The solution for the pressure in case (i) is

$$p = 2\mu \sum_{n=1}^{\infty} ne^{-ny} [(A_n + D_n) \sin nz - (B_n - C_n) \cos nz] \tag{17}$$

and in case (ii)

$$p = 2\mu \sum_{n=1}^{\infty} \frac{nK_0(ny)}{\phi(n)} [(K_1A_n + K_0D_n) \sin nz - (K_1B_n - K_0C_n) \cos nz]. \tag{18}$$

The stresses exerted by the body on the fluid are given by,

$$\sigma_{ij} = p\delta_{ij} - 2\mu e_{ij}, \tag{19}$$

where e_{ij} is the rate of strain tensor. They may be calculated from equations (11), (12), (13), (14), (17) and (18) for the velocities and pressures in the two cases considered. However, this requires tedious algebra, so the results will not be included here. We shall, however, include the rate of working per unit area of the sheet, which is defined by the following integral:

$$P = \int_{S_0} u_i \sigma_{ij} n_j \, dS, \tag{20}$$

where S_0 is a unit area of the mean tube.

To do this, the integral we will consider for a first approximation is

$$P = \frac{1}{2\pi} \int_{-\pi}^{\pi} [u\sigma_{zy} + v\sigma_{yy}]_{(z,\,a)} dz. \tag{21}$$

From this definition the rate of working per unit area in the two-dimensional case becomes (for non-dimensional k),

$$P = \mu \sum_{n=1}^{\infty} n(A_n^2 + B_n^2 + C_n^2 + D_n^2), \tag{22}$$

whereas in the axisymmetric flow model we obtain

$$P = \mu \sum_{n=1}^{\infty} n \left\{ 2(C_n B_n - A_n D_n) + \frac{1}{na}(C_n^2 + D_n^2) + \frac{1}{\phi(n)}[(K_1 A_n + K_0 D_n)^2 + (K_1 B_n - K_0 C_n)^2] \right\}. \tag{23}$$

It is difficult to define an efficiency parameter for these models. Tuck (1968) suggested taking the velocity of propulsion at fixed P, rather than fixed amplitude. However, we will define an efficiency parameter (i.e. a non-dimensional number) by

$$\eta = UT/P, \tag{24}$$

where U is the velocity of propulsion and P is the mean rate of working. T, a characteristic thrusting force per unit area is more difficult to define, since the total force exerted by the organism on the fluid is zero. In practice we take this as the simplest expression possible with the required dimensions $ML^{-1}T^{-2}$, and this is proportional to μU divided by the length of the metachronal wave. It may be noted, however, that a propulsive force, proportional to $\mu U/\lambda$, can be extracted from the equation for the surface stresses exerted on the fluid by the organism. There also exists a retarding force of equal magnitude, but opposite in sign to the propulsive force, thus giving a total force equal to zero. This point was illustrated in Taylor's (1951) paper for an infinite waving sheet, where the pressure force was balanced by the tangential stress exerted over the waving surface of the organism. However the efficiency is incurred, it is valuable in helping us to compare different modes of motion exhibited by the ciliated organisms.

3. Surface of organism

The oscillating surface envelope of the organism in the x co-ordinate system is defined by

$$\left.\begin{aligned} x_0 &= x + \epsilon \sum_{n=1}^{N} (a_n \sin n(kx + \sigma t) - b_n \cos n(kx + \sigma t)), \\ y_0 &= a + \epsilon \sum_{n=1}^{N} (c_n \sin n(kx + \sigma t) - d_n \cos n(kx + \sigma t)), \end{aligned}\right\} \tag{25}$$

where ϵ is suitably small and the coefficients a_n, b_n, c_n and d_n in the Fourier series expansions are $O(1)$. The above definitions of the surface envelope correspond to a progressive wave in the negative x direction with velocity magnitude $c = \sigma/k$, wavelength $2\pi/k$ and frequency $\sigma/2\pi$.

In the co-ordinate system used in the earlier section and with a non-dimensional wave-number (thus $c = \sigma$) the surface is defined by

$$\left.\begin{aligned} z_0 &= z + \epsilon \sum_{n=1}^{N} (a_n \sin nz - b_n \cos nz), \\ y_0 &= a + \epsilon \sum_{n=1}^{N} (c_n \sin nz - d_n \cos nz). \end{aligned}\right\} \tag{26}$$

The no-slip condition for this extensible sheet gives the following velocities at the surface envelope

$$\left.\begin{aligned} u(z_0, y_0) &= \sigma + \epsilon\sigma \sum_{n=1}^{N} n(a_n \cos nz + b_n \sin nz), \\ v(z_0, y_0) &= \epsilon\sigma \sum_{n=1}^{N} n(c_n \cos nz + d_n \sin nz). \end{aligned}\right\} \tag{27}$$

To obtain the previously defined surface velocity coefficients in (7), we take a Taylor series expansion for the velocity components about (z, a), which on rearrangement appears as

$$\begin{aligned} \mathbf{q}(z, a) &= \mathbf{q}^{(p+1)}(z, a) \\ &= \mathbf{q}(z_0, y_0) - \sum_{\substack{k=1 \\ k=m+n}}^{p} \binom{k}{m} \frac{(z_0 - z)^m (y_0 - a)^n}{k!} \left[\frac{\partial^k \mathbf{q}}{\partial z^m \partial y^n}\right]_{(z, a)} + O(\epsilon^{p+2}). \end{aligned} \tag{28}$$

To obtain the order of accuracy we require, an iterative technique is applied, which proceeds as follows.

For the first approximation (i.e. to $O(\epsilon)$) we need only equate $\mathbf{q}^{(1)}(z, a)$ to the no-slip conditions given in (27). This gives the following first-order approximations for A_n, B_n, C_n and D_n.

$$\left.\begin{aligned} &A_0 = \sigma, \\ &A_n = \epsilon n\sigma a_n, \quad B_n = \epsilon n\sigma b_n, \quad C_n = \epsilon n\sigma c_n, \quad D_n = \epsilon n\sigma d_n \quad (n = 1, 2, \ldots, N). \end{aligned}\right\} \tag{29}$$

It is apparent from these first-order solutions that the velocity of propulsion U is zero. To obtain net propulsion it is necessary to go to the second-order approximation, a conclusion reached by Taylor (1951).

To obtain the second-order approximations $O(\epsilon^2)$, we substitute the first-order approximations in the $k = 1$ terms on the right-hand side of (28). To calculate the velocity of propulsion the only second-order term we require is A_0, so we need only look at u, the velocity components in the z direction. Thus for the two-dimensional tube we obtain,

$$\begin{aligned} u(z, a) = \sigma &+ \epsilon\sigma \sum_{n=1}^{N} n(a_n \cos nz + b_n \sin nz) \\ &+ \epsilon^2\sigma \left[\sum_{n=1}^{N} (a_n \sin nz - b_n \cos nz) \sum_{n=1}^{N} n^2 (a_n \sin nz - b_n \cos nz) \right. \\ &\left. - \sum_{n=1}^{N} (c_n \sin nz - d_n \cos nz) \sum_{n=1}^{N} n^2 \{(c_n - 2b_n) \sin nz - (2a_n + d_n) \cos nz\} \right], \end{aligned} \tag{30}$$

which gives for the velocity of propulsion in dimensional form

$$U = \tfrac{1}{2}\epsilon^2\sigma k \sum_{n=1}^{N} n^2 [c_n^2 + d_n^2 - a_n^2 - b_n^2 + 2(a_n d_n - c_n b_n)]. \tag{31}$$

In the case of the infinite cylinder,

$$u(z,a) = \sigma + \epsilon\sigma \sum_{n=1}^{N} n(a_n \cos nz + b_n \sin nz)$$
$$+ \epsilon^2\sigma \Bigg[\sum_{n=1}^{N} (a_n \sin nz - b_n \cos nz) \sum_{n=1}^{N} n^2 (a_n \sin nz - b_n \cos nz)$$
$$+ \sum_{n=1}^{N} (c_n \sin nz - d_n \cos nz) \sum_{n=1}^{N} \frac{n^2}{\phi(n)} \{(2a_n K_1^2 + nad_n(K_1^2 - K_0^2)) \cos nz$$
$$+ (2b_n K_1^2 + nac_n(K_0^2 - K_1^2)) \sin nz\} \Bigg]. \tag{32}$$

The constant term in dimensional form gives for the velocity of propulsion,

$$U = \tfrac{1}{2}\epsilon^2\sigma k \sum_{n=1}^{N} n^2 \left[\frac{1}{\phi(n)} \{(K_1^2 - K_0^2) na(c_n^2 + d_n^2) + 2K_1^2(a_n d_n - b_n c_n)\} - a_n^2 - b_n^2 \right]. \tag{33}$$

It is worth noting that the velocity of propulsion in (33) is dependent on the tube radius as well as the amplitude parameters. This has the effect of making the y-directional amplitude parameter dependent on the tube radius for this small amplitude expansion to be valid.

We may calculate A_n, B_n, C_n and D_n to higher order. In the general case we find that,

$$\left.\begin{aligned} U &= -A_{0j}\epsilon^j \quad (j = 2, 4, \ldots), \\ A_n = A_{nj}\epsilon^j, \quad B_n &= B_{nj}\epsilon^j, \\ C_n = C_{nj}\epsilon^j, \quad D_n &= D_{nj}\epsilon^j, \end{aligned}\right\} \quad (j, n = 1, 2, 3, \ldots), \tag{34}$$

where A_{nj}, B_{nj}, C_{nj} and D_{nj} are functions of a_n, b_n, c_n and d_n. To obtain solutions to order M, it is necessary for us to take $p = M - 1$ in (28), and to have first-order substitutions in the $k = M - 1$ terms down to $M - 1$ order approximations for the coefficients in the $k = 1$ terms. This then assures accuracy to order ϵ^M in (34). This technique is especially simple and easy to calculate to low orders of approximation, but becomes tedious for higher-order approximations for the general cases considered so far. However for special cases (next section) we have worked to fourth order for the velocities of propulsion.

4. Applications to ciliary propulsion

The beat of a single cilium can be separated into two distinct phases, one phase being the effective stroke (when the cilium beats in the opposite direction to propulsion of the body) and the other phase the recovery stroke. The classical case of an effective beat is when the cilium beats nearly rigidly in its effective stroke, but retreats limply during the recovery stroke. Generally the recovery stroke takes far longer than the effective beat. For this model of ciliary propulsion to be valid we need the cilium to beat in the same direction as the wave is progressing (symplectic metachronism), as in this case the cilia are close together throughout the whole beat. *Opalina* exhibits this type of metachronism and its beat is illustrated in figure 2(*b*). Its effective and recovery strokes vary

considerably from the classical model illustrated in figure 2(*a*), but we can still distinguish the two strokes. The path traced out by the tips of the cilia in *Opalina* is approximately elliptical in shape.

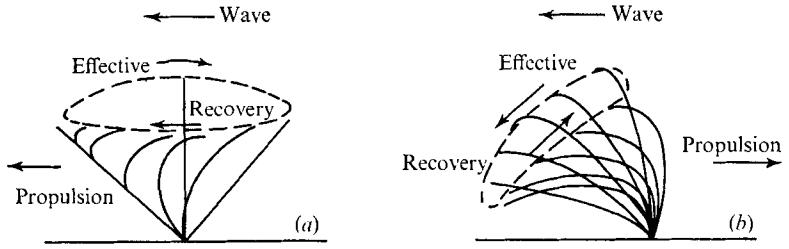

FIGURE 2. (*a*) Classical beat of a cilium; showing effective and recovery strokes (*Paramecium*). (*b*) Beat of *Opalina*.

In this section the path of a tip of a cilium will be matched onto the movement of each point of the waving sheet. Sleigh (1968) has obtained numerous data on the movement of tips of cilia, and approximations will be made using these plotted paths. The models we will use can be represented by (in the x co-ordinate system)

$$\left.\begin{aligned} x_0 &= x+\beta\cos(kx+\sigma t)+\gamma\sin(kx+\sigma t),\\ y_0 &= a+b\sin(kx+\sigma t). \end{aligned}\right\} \tag{35}$$

This definition for the surface envelope of the tube gives for each labelled point a path through which it traverses in each period of oscillation (in much the same way as a fluid particle in a water wave). Normally it is found that the axis of the locus of a tip of a cilium is inclined to the body axis, this being the reason for the inclusion of γ in (35).

For the surface defined by (35), the following velocities (second order) and rates of working (first order) are obtained for cases (i) and (ii):

For (i)
$$U = \tfrac{1}{2}\sigma k(b^2+2b\beta-\beta^2-\gamma^2), \tag{36}$$

with rate of working
$$P = \mu\sigma^2 k(b^2+\beta^2+\gamma^2); \tag{37}$$

and for (ii)
$$U = \tfrac{1}{2}\sigma k\,[(1/\phi(a))\{[K_1^2(a)-K_0^2(a)]ab^2+2K_1^2(a)\,b\beta\}-\beta^2-\gamma^2] \tag{38}$$

and
$$P = \mu\sigma^2 k\left[\frac{b^2}{ka}-2b\beta+\frac{1}{\phi(a)}\{K_1^2(a)\gamma^2+[K_1(a)\beta+K_0(a)b]^2\}\right]. \tag{39}$$

It is found that as the radius of the axisymmetric cylinder increases, the velocity of propulsion tends to that of the infinite flat sheet. A graph comparing $U/\frac{1}{2}c(bk)^2$ for the two models as the radius a increases is shown in figure 3. We will now discuss the two cases separately, and compare them with results obtained previously.

Case (i)

From (36) we note several results obtained previously, namely by Taylor (1951) and Tuck (1968). Taylor considered the inextensible model with $b \neq 0$, β and γ zero, and obtains for a velocity of propulsion,

$$U = \tfrac{1}{2}\sigma k b^2 = \tfrac{1}{2}c(kb)^2,$$

whereas Tuck obtains for the problem with $\beta \neq 0$, b and γ zero, a velocity of propulsion,

$$U = -\tfrac{1}{2}\sigma k\beta^2 = -\tfrac{1}{2}c(k\beta)^2.$$

It should be pointed out that the extensibility condition does not have any effect on the velocities of propulsion until fourth order, so the results obtained to second order of accuracy compare exactly with Taylor's and Tuck's results. However, on working to fourth order, differences from those calculated by Taylor are noted.

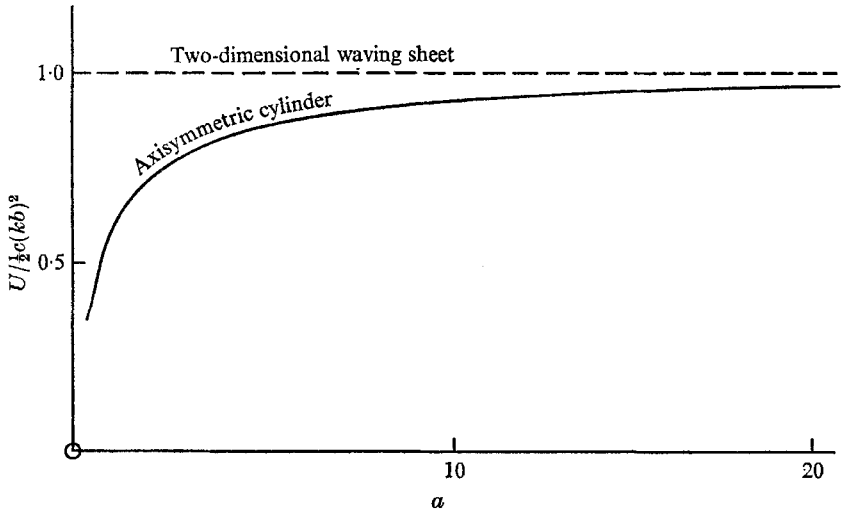

FIGURE 3. Graph comparing the velocities of propulsion for increasing radius for the two infinite models (transverse motions only).

From these observations we note that transverse and longitudinal oscillations tend to propel the sheet in opposite directions. However if we combine the two cases we find that

$$U = \tfrac{1}{2}\sigma k(b^2 + 2\beta b - \beta^2). \tag{40}$$

The first two terms in (40) correspond to the result obtained by Reynolds (1965), for straining of the surface, as, to first-order Reynolds δ corresponds to β in this analysis. This particular case defines for each labelled point (x, a) a path which is that of an ellipse, with axes of length b and β in the y and x directions respectively. For the case of the circular path ($\beta = b$, optimal velocity for β and b both less than a constant determined later), it is found that the direction of propulsion relative to the wave is dependent on whether the tip moves in an anticlockwise or clockwise direction, the direction of propulsion being opposite to the direction of movement of the tip on the upper part of the path (for $y \geqslant a$). Thus, if the tip moves in an anticlockwise direction, $U = c(kb)^2$, whereas in the clockwise direction $U = -c(kb)^2$. From this solution (40) it is noticed that organisms which have predominantly transverse motions (e.g. *Opalina*) are propelled in an opposite direction to the metachronal wave, whereas predominant longitudinal movements (e.g. *Paramecium*) tend to propel the organism in the same direction as

the wave. However in this latter case, we do not wish to suggest that this analysis is a correct model for this organism, but it is worth noting the apparent connexion with observations between the path of movement of the tip and the type of metachronism.

Before any comparisons can be made, it is necessary to know the validity of the preceding analysis, and, as this is a small-amplitude perturbation technique, the limit of the size of ϵ or in these specific cases the limitations in magnitude on β, γ and b. The fourth-order approximation to (40) is,

$$U = \tfrac{1}{2}\sigma k[(b^2+2\beta b-\beta^2-\gamma^2) - k^2(b^4+\tfrac{1}{2}b^3\beta-2b^2\beta^2+\tfrac{1}{2}b\beta^3-2b^2\gamma^2+\tfrac{1}{2}b\beta\gamma^2)]. \quad (41)$$

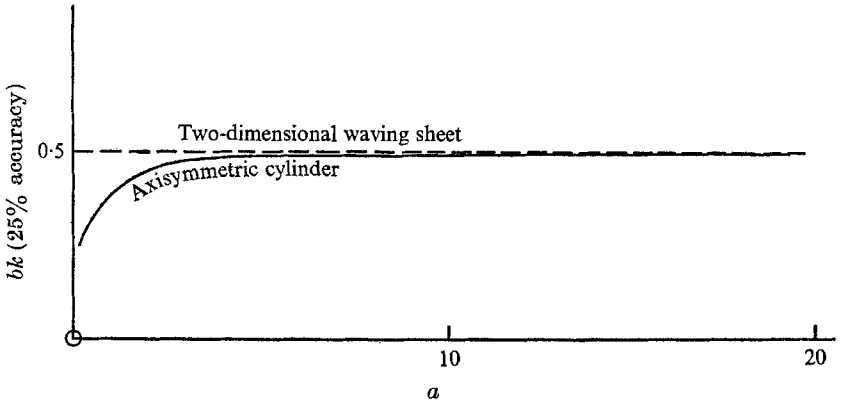

FIGURE 4. Graph illustrating the dependence of maximum value of amplitude parameter bk on the radius a, for axisymmetric cylinder model.

If we take the criterion of Taylor (1951), allowing an error of 25%, this then allows us to take (for equal displacements in both normal and tangential directions)

$$\left.\begin{aligned} bk &= \tfrac{1}{2}, \\ k(\beta^2+\gamma^2)^{\frac{1}{2}} &= \tfrac{1}{2} \quad \text{for} \quad |\beta| > \tfrac{1}{6}. \end{aligned}\right\} \quad (42)$$

For the case of *Opalina* this upper limit coincides with that experienced by the organism, so an approximation can be made.

Case (ii)

In this model it is found that the magnitude of the amplitude parameter b in the y direction is dependent on the tube radius. To show this dependence, the simplest example of pure transverse motion is taken. A graph showing the change of b with a, allowing for a 25% variation from the second-order velocity of propulsion is shown in figure 4. Again it is shown that b tends to $\frac{1}{2}$; that expected in the infinite flat sheet model. The amplitude of longitudinal movements, however is not dependent on the tube radius.

From the definition of the efficiency parameter (24), we obtain the following formulation in the case of the infinite waving sheet with U defined in (36), P in

(37) and $T = 2\mu kU$. If we include k with b, β and γ to make them non-dimensional, we obtain

$$\eta = \frac{1}{2}\frac{(b^2+2b\beta-\beta^2-\gamma^2)^2}{b^2+\beta^2+\gamma^2}. \tag{43}$$

As the infinite cylinder tends to the infinite sheet as the radius a increases, we need only take this efficiency into consideration.

The maximum efficiency occurs when $\gamma = 0$ and $\beta = 0{\cdot}6b$ (or $b = -0{\cdot}6\beta$), which for $b = \frac{1}{2}$ (or $\beta = \frac{1}{2}$) gives an efficiency $\eta = 31\,\%$. In other words minimum power output is found when the tips describe an ellipse with axis ratio of 0·6. The maximum velocity occurs when $b = |\beta|$, $\gamma = 0$, and has an efficiency of 25 %.

It should be emphasized that these efficiencies are very much dependent on the definition in (24). Previous calculated efficiencies have been taken in comparison with inert bodies, so therefore these efficiencies quoted are far higher than those, for example, in Blake (1971) for the spherical model.

5. Comparisons with the spherical model

A comparison of the velocities of propulsion for the infinite models of this paper and the axisymmetric spherical model (Blake 1971) are discussed in this section. As the infinite cylinder results tend to that for the flat sheet as the radius increases, we need only take into consideration those of the flat sheet.

Recalling the notation for the spherical body, and considering only radial (transverse) oscillations we define the surface by

$$R = a[1+\epsilon\gamma(N)\{\cos\sigma t[P_{N-2}(\cos\theta)-P_N(\cos\theta)] + \sin\sigma t[P_{N-3}(\cos\theta)-P_{N-1}(\cos\theta)]\}]. \tag{44}$$

$P_N(\cos\theta)$ are Legendre polynomials, and $\gamma(N)$ is chosen such that the maximum perturbation of the radius is $a\epsilon$ (i.e. amplitude of wave). The velocity of propulsion for this model is

$$\left.\begin{aligned} U &= a\sigma\epsilon^2\gamma^2(N)\,F(N), \\ \text{where} \qquad F(N) &= \sum_{n=N-3}^{N-1}\frac{n^2-n-\frac{1}{2}}{(2n+1)\,(2n+3)}. \end{aligned}\right\} \tag{45}$$

For this model the relevant parameter is ϵN, which we may equate to kb of the infinite models. If we define the wave velocity $c = a\sigma/N = \sigma/k$ for the two models, we have the following velocities of propulsion:

$$\left.\begin{aligned} &U = \tfrac{1}{2}c(kb)^2; \quad \text{for the infinite waving sheet model,} \\ \text{and} \qquad &U = \frac{\gamma^2(N)F(N)}{N}\,c(\epsilon N)^2; \quad \text{for the axisymmetric sphere.} \end{aligned}\right\} \tag{46}$$

Thus for a comparison we need only look at $\gamma^2(N)\,F(N)/N$ to see how it compares with $\frac{1}{2}$.

As N increases it can be shown that the velocity of propulsion in the spherical case is 40–45 % that of the infinite flat sheet. This is an encouraging result as

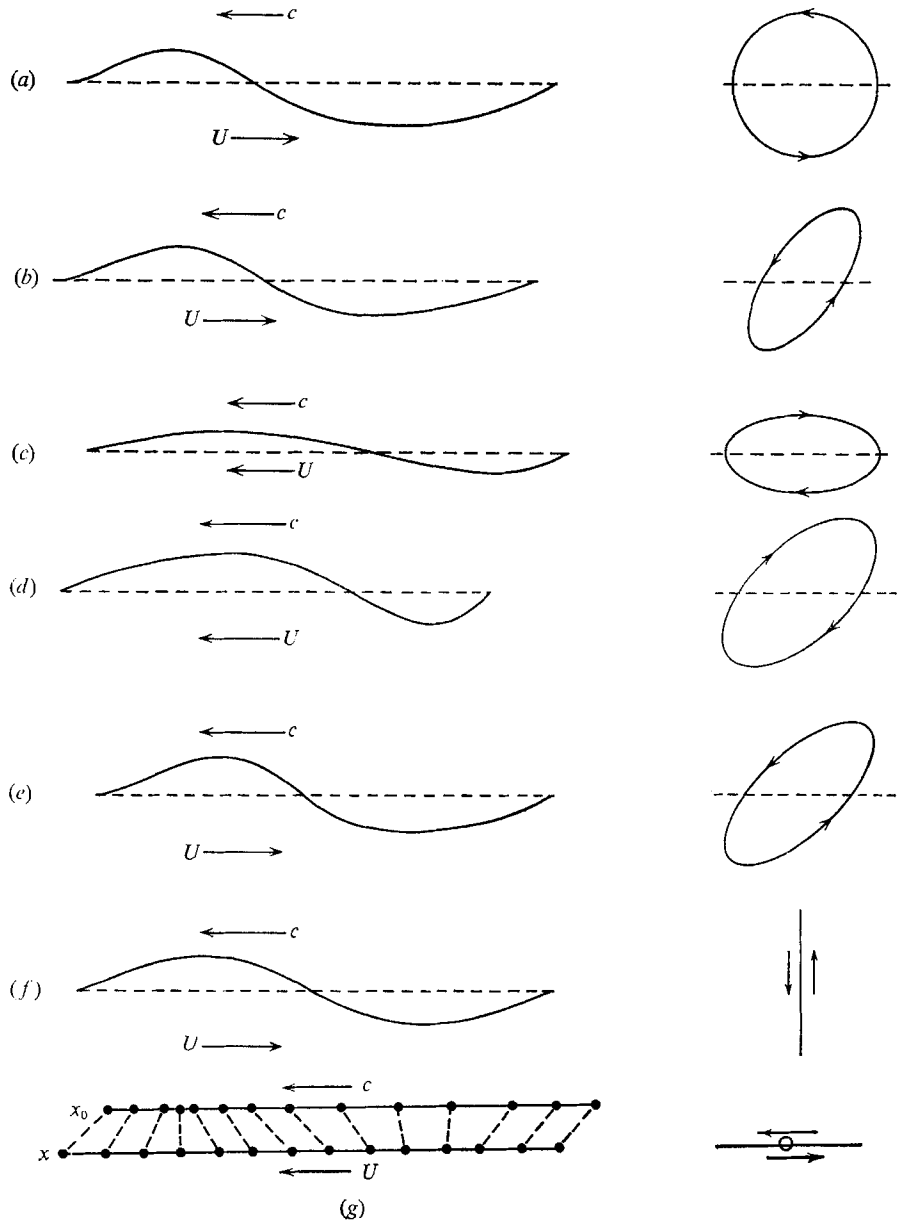

FIGURE 5. Graphs showing surface envelope shapes, and particle paths for varying β, γ and b. The corresponding efficiency η and velocity of propulsion U of organism in comparison to wave speed c are given.

	β	γ	b	U/c	η
(*a*)	0·5	0	0·5	0·25	25 %
(*b*)	0·25	0·25	0·5	0·19	19 %
(*c*)	−0·5	0	0·25	−0·22	30 %
(*d*)	−0·4	0·3	0·5	−0·2	16 %
(*e*)	0·3	0·4	0·5	0·15	9 %
(*f*)	0	0	0·5	0·125	12·5 %
(*g*)	0·5	0	0	−0·125	12·5 %

a spherical organism is not an ideal shape for ciliary propulsion at low Reynolds number, because cilia near the front and rear are not beating in a direction favourable for propulsion. Previously it was remarked that ciliated organisms tend to be elongated or flat, so for these bodies a solution between that of the finite sphere and infinite sheet would be anticipated. It also may help to dispel some of the natural doubts as to whether the infinite oscillating sheet is a poor model for propulsion at low Reynolds number.

6. Models and examples for *Opalina*

In this section graphs showing the shape of the progressive wave, the path of each point of the sheet, velocities of propulsion and efficiency are shown. A model as close as possible to that of *Opalina* gives a velocity of propulsion $U = 0{\cdot}19c$, where c is the wave velocity. The velocities obtained are comparable to those of *Opalina*, whose velocity of propulsion is $O(100\,\mu\text{m/sec})$ and wave speed $c = 200$–$400\,\mu\text{m/sec}$. It can be seen that by introducing the longitudinal oscillations the resulting shape of the wave is considerably distorted from that of the sinusoidal wave used by previous authors. In conclusion, this approach appears to be a reasonable approximation to ciliary propulsion for a symplectic metachronal wave, allowing comparison between the numerous modes.

This work was carried out while the author was in receipt of a George Murray Scholarship from the University of Adelaide, and a studentship from C.S.I.R.O. of Australia. Comments and suggestions from Professor M. J. Lighthill are acknowledged.

REFERENCES

BLAKE, J. R. 1971 A spherical envelope approach to ciliary propulsion. *J. Fluid Mech.* **46**, 199–208.

BURNS, J. &. PARKES, T. 1967 Peristaltic motion. *J. Fluid Mech.* **29**, 731–743.

LIGHTHILL, M. J. 1952 On the squirming motion of nearly spherical deformable bodies through liquids at very small Reynolds numbers. *Comm. Pure Appl. Math.* **5**, 109–118.

REYNOLDS, A. J. 1965 The swimming of minute organisms. *J. Fluid Mech.* **23**, 241–260.

SLEIGH, M. A. 1968 Patterns of ciliary beating. *Symp. Soc. exp. Biol.* **22**, 131–150.

TAYLOR, G. I. 1951 Analysis of the swimming of microscopic organisms. *Proc. Roy. Soc.* A **209**, 447–461.

TAYLOR, G. I. 1952 The action of waving cylindrical tails in propelling microscopic organisms. *Proc. Roy. Soc.* A **211**, 225–239.

TUCK, E. O. 1968 A note on a swimming problem. *J. Fluid Mech.* **31**, 305–308.

WATSON, G. N. 1966 *A treatise on theory of Bessel functions.* Cambridge University Press.

WEINSTEIN, A. 1953 Generalized axially symmetric potential theory. *Bull. Amer. Math. Soc.* **59**, 20–28.